Fundamental Toxicological Sciences (Fundam. Toxicol. Sci.)
Vol.11, No.3, 109-121, 2024

The Japanese Society of Toxicology

Fundamental Toxicological Sciences

URL : http://www.fundtoxicolsci.org/index_e.html

Original Article

Effect of differently coated titanium dioxide nanoparticles on the lung in wild-type and Nrf2 null mice

Ryoya Takizawa[1], Akihiko Ikegami[1], Cai Zong[2], Syun Nemoto[2], Yuki Kitamura[1], Nathan Mise[1], Gaku Ichihara[2] and Sahoko Ichihara[1]

[1]*Department of Environmental and Preventive Medicine, Jichi Medical University School of Medicine, Shimotsuke, Japan*
[2]*Department of Occupational and Environmental Health, Tokyo University of Science, Noda, Japan*

(Received May 10, 2024; Accepted May 19, 2024)

ABSTRACT — Nanoparticles (NPs) are used in a variety of fields, including industry, medicine, and food production. Predicting the potential toxicity and biological effects of NPs is challenging due to the influence of their physicochemical properties, such as particle shape and coating constituents. This study investigated the pulmonary effects of differently coated titanium dioxide (TiO_2) NPs in wild-type and nuclear factor erythroid 2-related factor 2 (Nrf2) null mice. C57BL6/J wild-type and Nrf2 null mice were exposed to uncoated TiO_2 NPs, or NPs coated with either hydroxide aluminum, or with aluminum hydroxide/stearic acid. After a two-week exposure period, no significant changes were observed in lung weight, cell counts of bronchoalveolar lavage fluid, mRNA levels of proinflammatory cytokines, and antioxidant gene expression in either mouse strain. In addition, human lung carcinoma A549 cells exposed to three types of TiO_2 NPs showed no significant changes in cell viability, cytotoxicity, or intracellular reactive oxygen species production. These findings suggest that the toxicity of the TiO_2 NPs, regardless of surface modification, is minimal to the respiratory system of mice and human alveolar epithelial cells.

Key words: Nanomaterial, Titanium dioxide, Inflammation, Respiratory system, Nrf2, Reactive oxygen species

INTRODUCTION

With the advancement of nanotechnology, nanoparticles (NPs) have found applications in diverse fields, including industry, medicine, and food (Chaudhry *et al*., 2008). Titanium dioxide nanoparticles (TiO_2 NPs) are the most widely used NPs globally, and are used extensively in the production of cosmetics, sunscreens, and food colorants (Baranowska-Wojcik *et al*., 2020; Piccinno *et al*., 2012). Consequently, the prevalence of exposure to TiO_2 NPs has increased. However, the health risks associated with TiO_2 NP exposure remain unclear.

Bettini *et al*. (2017) reported that E171, a TiO_2 NP that is widely used as a food colorant, was potentially carcinogenic in the rat colon. In 2020, France banned the use of TiO_2 NPs in food products due to concerns about the safety of TiO_2 NP exposure through consumption. In 2021, the European Food Safety Authority (EFSA) published an opinion stating that the effects of TiO_2 NP exposure are unclear and that their consumption cannot be considered safe (Bampidis *et al*., 2021; Baranowska-Wojcik *et al*., 2020). The discussion about TiO_2 NPs toxicity is ongoing, and public interest is focused on clarifying whether TiO_2 NPs are safe.

One of the major characteristics of NPs is their small particle size (<100 nm). It has been proposed that NPs,

Correspondence: Sahoko Ichihara (E-mail: saho@jichi.ac.jp)

which are smaller in size than particulate matter $(PM)_{2.5}$, can penetrate deeper into lungs more easily and are therefore considered to have higher health risks (Johnson *et al*., 2021; Thangavel *et al*., 2022). The inhalation of NPs occurs in many workplaces, especially in factories that handle NPs (Ichihara *et al*., 2016).

Compared to larger particles, the small size of NPs means that they have a relatively larger surface area to volume ratio. This large surface area to volume ratio contributes to the mechanical strength of NPs, thereby facilitating the application of TiO_2 NPs as biocompatible materials (Suttiponparnit *et al*., 2011). However, these structural characteristics can also facilitate molecular interactions, leading to the production of reactive oxygen species (ROS), DNA damage, and disruption to cell membranes (Najahi-Missaoui *et al*., 2020). Consequently, assessments of NP toxicity should be described not only in terms that are relative to their weight, but also their surface area, as the surface activity of NPs markedly influences their biological effects. In addition to their influence on the surface reactivity and the cellular uptake of NPs, surface charges also affect the cytotoxicity of NPs and their dispersion in solvents (Bhattacharjee, 2016). NPs exist in various shapes such as spherical, cubic, fibrous, rod-like, elliptical, cylindrical, and two-dimensional sheet-like structures (Zhang *et al*., 2015). Like surface charge, these differences in shape also influence the dispersion of NPs in solvents and NP toxicity. In particular, it has been reported that fibrous nanoparticles such as TiO_2 nanobelts induce inflammation in mouse alveoli (Hamilton *et al*., 2009).

It has been proposed that the surface coating of NPs is an important factor affecting NP toxicity. Changes in the surface coating of NPs have been demonstrated to alter their physical properties, *in vivo* kinetics, and biosafety (Najahi-Missaoui *et al*., 2020; Takechi-Haraya *et al*., 2022). For example, surface coatings on silica NPs have been reported to alter the inflammatory responses and extent of DNA damage in cells and lung tissues (Inoue *et al*., 2021; Yoshida *et al*., 2012). Since many of the NPs that are used in a variety of applications have surface coatings, assessing the contribution of these surface coatings to NP toxicity is important.

Numerous NPs are also capable of causing oxidative stress, which can in turn induce inflammation and cell death (De Stefano *et al*., 2012). Nuclear factor erythroid 2-related factor 2 (Nrf2) is a transcription factor that responds to oxidative stress by increasing the expression of antioxidant enzymes (Bellezza *et al*., 2018). For example, exposure of Nrf2 null ($Nrf2^{-/-}$) mice to zinc oxide (ZnO) NPs increased pro-inflammatory cytokines and chemokines (Sehsah *et al*., 2022). In addition, exposure to TiO_2 NPs has been shown to increase ROS levels in human lung carcinoma A549 cells, the HepG2 human liver cancer cell line, and cells in the liver, kidney, and brain of mice (Sayes *et al*., 2006; Zhang *et al*., 2010). Furthermore, it has been reported that Nrf2 deletion increased TiO_2 NP-induced DNA damage in HepG2 cells and mouse kidney cells (Shi *et al*., 2015).

The present study investigated the effects of TiO_2 NP surface coatings on lung inflammation in $Nrf2^{-/-}$ mice and wild-type mice, as well as their cytotoxicity to type II alveolar epithelial cells.

MATERIALS AND METHODS

TiO_2 nanoparticles

Three types of TiO_2 NPs (LU-572-2, TTO-S-3, TTO-S-4) with different surface coatings were obtained from ISHIHARA SANGYO KAISHA (Osaka, Japan): LU-572-2 (LU) is uncoated, TTO-S-3 (S3) is coated with aluminum hydroxide, and TTO-S-4 (S4) is coated with aluminum hydroxide and stearic acid. The TiO_2 NPs, which have the same primary diameter of 15 nm and rutile crystal structure, were dispersed and their hydrodynamic sizes were then measured using methods described previously (Tada-Oikawa *et al*., 2016). TiO_2 NPs were dispersed in dispersion medium (DM), cell culture medium, or distilled water. The composition of the DM is the same as that described previously (Wu *et al*., 2014). Briefly, DM consists of Ca^{2+} and Mg^{2+} free phosphate buffered saline (PBS, pH 7.4; Thermo Fisher Scientific, Waltham, MA), supplemented with 5.5 mM D-glucose (Sigma-Aldrich, St. Louis, MO), 0.6 mg/mL bovine serum albumin (Sigma-Aldrich), and 0.01 mg/mL 1,2-dipalmitoyl-sn-glycero-3-phosphocholine (DPPC) (Sigma Aldrich). The NPs were dispersed using a cup-type sonicator (model 450, Branson Sonifier, Danbury, CT) set at 80% pulsed mode, 100 W, and 15 min. After dispersion in DM, cell culture medium or distilled water, the hydrodynamic size and Z-average of the NPs were determined using dynamic light scattering (DLS) technology with a Zetasizer Nano-S (Malvern Instruments, Worcestershire, UK). Zeta potentials were also measured using a Zetasizer Nano ZSP (Malvern Instruments).

Transmission electron microscope (TEM) image analysis

TiO_2 NPs were dispersed in distilled water to a dilution of 25 μg/mL. Then, 50 μL of TiO_2 NPs were mounted on a grid (elastic wettie ELW-C075, Okenshoji, Tokyo, Japan), dried in a desiccator, and observed under a TEM

(HT7700; Hitachi, Japan, Tokyo) operated at an accelerating voltage of 80 kV and ×100,000 magnification.

Study animals

Nrf2$^{-/-}$ mice (10 weeks old, 22-29 g) were reared (Itoh *et al*., 1997) and backcrossed more than six times. Wild-type C57BL/6JJcl mice (10 weeks old, 22-29 g) were purchased from CLEA Japan (Tokyo, Japan). Nrf2$^{-/-}$ mice and wild-type mice were weighed and randomly divided into three groups, respectively (n = 8 in each group). All of the mice were housed and acclimatized in a clean environment for 1 week before starting the exposure treatments. Food and water were provided ad libitum. The animal room was light- and temperature-controlled and mice were maintained under a 12-hr light-dark cycle (lights on at 9:00 and off at 21:00) at a room temperature of 23–25°C, and a relative humidity of 57–60%. The experiments adhered to the guidelines outlined in the Japanese Act Concerning Protection and Control of Animals and the Animal Experimentation Guidelines of Jichi Medical University. The experiment protocol was approved by the Jichi Medical University Animal Experiment Committee (#21038-03).

Pharyngeal aspiration of NPs

Following the methods established for pharyngeal aspiration in a previous study (Sehsah *et al*., 2019), mice were anesthetized by intraperitoneal injection of a mixed anesthesia. The anesthesia was prepared by supplementing saline (Otsuka Pharmaceutical Factory, Tokushima, Japan) with 30 μg/mL medetomidine hydrochloride (Domitor; ZENOAQ, Fukushima, Japan), 400 μg/mL midazolam (Sandoz; Basel, Switzerland), and 500 μg/mL of butorphanol tartrate (Vetorphale; Meiji Seika Pharma, Tokyo, Japan). After induction of anesthesia, the mouse was positioned on an inclined board with its upper incisors secured using a rubber band. The mouse's tongue was then gently extended from the oral cavity using blunt forceps, and a 40 μL aliquot of NP suspension was placed at the back of tongue. Then the tongue was held in this position for 1 min to facilitate inhalation of the NPs (Suzuki *et al*., 2016). Following this procedure, the mouse was injected intraperitoneally with 30 μg/mL atipamezole hydrochloride (Antisedan; Espoo, Finland) to reverse the anesthesia. The mouse was then placed on a heated plate maintained at 37°C until it recovered from the anesthesia. Mice were exposed to TiO_2 NPs dispersed in DM at concentrations of 10 μg (low concentration) and 30 μg (high concentration), which are equivalent to 0.5 mg/kg and 1.5 mg/kg body weight, respectively. The lower concentration of 0.5 mg/kg is comparable to the estimated lung deposition of 0.58 mg/kg of workers exposed to fine TiO_2 particles at the recommended exposure limit (REL) of 2.4 mg/m^3 set by National Institute for Occupational Safety and Health. This exposure scenario assumes a full deposition of fine TiO_2 particles inhaled in a ventilation volume of 500 mL at a breathing rate of 12 breaths/min over an 8-hr workday for five consecutive days.

Bronchoalveolar lavage fluid (BALF)

Two weeks following exposure to TiO_2 NPs, BALF was collected from each mouse. After being anesthetized by intraperitoneal injection of a mixture of three anesthetics, bronchoalveolar lavage (BAL) was performed by cannulating the trachea with a 20-gauge needle, followed by the injection and subsequent collection of PBS (FUJIFILM Wako Pure Chemical, Osaka, Japan) into/from both lungs. This operation was repeated three times to collect of total of 2 mL of BALF. The collected BALF was centrifuged at 1500 rpm for 5 min at 4°C. After centrifugation, the supernatant was aliquoted into two tubes and stored at -80°C. The cell pellets were re-suspended in 1 mL of ACK Lysing Buffer (Thermo Fisher Scientific) and incubated for 5 min at room temperature. Then, 10 mL of cold PBS was added and centrifuged at 1500 rpm for 5 min at 4°C. The resulting cell pellets were then resuspended using 0.5 mL of PBS, and the total number of cells was counted using a hemocytometer (TC20, Bio-Rad, Hercules, CA). The remaining re-suspended cells were concentrated and deposited on glass slides using a Cytospin™ Centrifuge (EZ Single Cytofunnel White, Epredia, Portsmouth, NJ), followed by Diff-Quik staining (Sysmex, Hyogo, Japan). The BALF macrophages, granulocytes, and lymphocytes were identified under a microscope (FSX100, Olympus, Tokyo, Japan) and the number of each cells was counted using a ×20 objective lens across 10 fields. Total BALF protein levels were measured using a Pierce™ BCA Protein Assay Kit (Thermo Fisher Scientific), following the manufacturer's instructions.

Dissection, measurement of organ weights, and histological analysis

After collecting BALF, mice were euthanized and dissected, and the weights of different organs (lungs, heart, liver, spleen, adrenal glands, and kidneys) were recorded. Subsequently, sections of the organs were fixed in 4% paraformaldehyde (FUJIFILM Wako Pure Chemical). Specifically, a section of the middle of the left lung was fixed and embedded in paraffin (Sigma-Aldrich). These paraffin-embedded lung tissues were then cut into

5 μm-thick sections using a rotary microtome (HM360, Marshall Scientific, Hampton, NH), and stained with hematoxylin and eosin (H&E) for histological examination. Following staining, the lung tissues were observed under a light microscope (BX63, Olympus).

Quantitative real-time polymerase chain reaction (RT-PCR) analysis

Total RNA was extracted from frozen lung tissues using an SV Total RNA Isolation system (Promega, Madison, WI) and the RNA concentrations were measured using a Nanodrop-1000 spectrophotometer (ver. 3.5.1; Thermo Fisher Scientific). Complementary DNA was synthesized using SuperScript™III reverse transcriptase (Thermo Fisher Scientific). Quantitative real-time PCR was performed using an AriaMX real-time PCR system (Agilent Technologies, Santa Clara, CA). The gene expression of Nrf2-related factors, such as superoxide dismutase 1 (SOD1), heme-oxygenase 1 (HO-1), and NAD(P) H quinone oxidoreductase (NQO1), was quantified. In addition, the expression levels of inflammatory cytokines, interleukin-6 (IL-6) and tumor necrosis factor alpha (TNF-α), were measured. Gene expression levels were normalized to the β-actin gene. The sequences of the primers used were as follows: SOD1 (NM_011434.1): CAGGACCTCATTTTAATCCTCAC (Forward) and TGCCCAGGTCTCCAACAT (Reverse); HO-1 (NM_010442.2): AGGCTAAGACCGCCTTCCT (Forward) and TGTGTTCCTCTGTCAGCATCA (Reverse); NQO1 (NM_008706.5): AGCGTTCGGTATTACGATCC (Forward) and AGTACAATCAGGGCTCTTCTCG (Reverse); IL-6 (NM_031168.2): GCTACCAAACTGGATATAATCAGGA (Forward) and CCAGGTAGCTATGGTACTCCAGAA (Reverse); TNF-α (NM_013693.2): TCTTCTCATTCCTGCTTGTGG (Forward) and GGTCTGGGCCATAGAACTGA (Reverse); and β-actin (NM_007393.3): AAGGCCAACCGTGAAAAGAT (Forward) and GTGGTACGACCAGAGGCATAC (Reverse).

Cell cultures

Human lung carcinoma A549 cells were obtained from the Japanese Collection of Research Bioresources Cell Bank (JCRB, Osaka, Japan). The A549 cells were cultured in Eagle's Minimum Essential Medium (E-MEM, FUJIFILM Wako Pure Chemical) supplemented with 10% fetal bovine serum (FBS, Biowest, Riverside, MO) and MEM non-essential amino acids (MEM NEAA, Thermo Fisher Scientific) at 37°C in an atmosphere of 5% CO_2. The A549 cells were seeded in T25 flasks (Sumitomo Bakelite Co, Tokyo, Japan) and passaged every 2–3 days. Before passaging, A549 cells were detached using Trypsin-EDTA (Thermo Fisher Scientific).

Cell viability assay

A549 cells were seeded at a density of 2.5×10^4 cells/well in 96-well plates and cultured for 24 hr at 37°C in a 5% CO_2 atmosphere. TiO_2 NPs were dispersed in the culture medium to achieve final concentrations ranging from 1 to 100 μg/mL. After 24 hr incubation with each TiO_2 NP, cell viability was measured using two methods: an MTS assay using CellTiter 96® AQueous One Solution (Promega), and an LDH assay using a Cytotoxicity LDH Assay Kit-WST (DOJINDO, Kumamoto, Japan). After exposure to each of the NPs, the supernatants were removed, and the cells were incubated for 1 hr in fresh medium containing MTS reagent. After incubation, 100 μL of the supernatant was transferred to another 96-well plate for absorbance measurement at 490 nm with a plate reader (SH-1300Lab Microplate Reader; Corona Electric, Ibaraki, Japan). For the LDH assay, after removing the initial supernatant, cells were transferred to another 96-well plate and incubated with an equal volume of LDH assay reagent. After 1 hr incubation, the absorbance was measured at 490 nm with a plate reader (SH-1300Lab Microplate Reader).

Measurement of ROS

Reactive oxygen species were quantified using an OxiSelect™ Intracellular ROS assay kit (Cell Biolabs, San Diego, CA) following the manufacturer's instructions. Briefly, A549 cells were seeded at a density 2.5×10^4 cells/well in black 96-well plates (Sumitomo Bakelite) and cultured for 24 hr at 37°C in a 5% CO_2 atmosphere. Then, the medium containing DCFH-DA reagent was added, and the cells were incubated for 30 min at 37°C in a 5% CO_2 atmosphere. After incubation, the supernatant was removed, and the cells were exposed to different concentrations of TiO_2 NPs at 37°C in a 5% CO_2 atmosphere. Fluorescence was measured at time intervals of 1, 3, 6, and 12 hr using fluorescence plate reader (2030 ARVOTM X One, PerkinElmer, Waltham, MA) at excitation/emission wavelengths of 485 nm/535 nm.

Statistical analysis

Data are presented as mean ± standard deviation (SD). Comparisons among three groups were conducted using one-way analysis of variance (ANOVA) followed by Tukey-Kramer multiple comparison test using R version 3.6.1 (R Foundation for Statistical Computing, Vienna, Austria). The same test was applied to analyze the data of the organ weight of mice, cells in BALF, and mRNA expression in lung. A p-value <0.05 was considered to indicate

statistical significance. For comparisons between wild-type and Nrf2$^{-/-}$ mice, the Student's *t*-test was employed, also using R version 3.6.1.

RESULTS

Characterization of TiO_2 NPs

Three types of TiO_2 NPs were visualized by TEM (Fig. 1). Vertically elongated shapes were consistently observed across all TiO_2 NPs and there were no discernable differences in shape among the three TiO_2 NPs. The primary particles of all TiO_2 NPs exhibited a short axis of approximately 15 nm and a long axis of approximately 100 nm.

The hydrodynamic size, PdI, and zeta potential of three types of TiO_2 NPs in distilled water, DM, and cell culture medium were estimated using the DLS method (Table 1). In distilled water, the hydrodynamic size of LU TiO_2 NPs was significantly larger than that of S3 and S4. The hydrodynamic size of S4 was significantly larger than that of S3. A similar pattern was observed for the PdI of the three NPs. The zeta potential of LU was significantly lower than that of S3 and S4. When TiO_2 NPs were dispersed in DM, the hydrodynamic size of LU was approximately 100 nm, whereas S3 and S4 were approximately 150 nm. The hydrodynamic size of LU in DM was significantly smaller than that of S3 and S4. The PdI of LU was larger than that of S3 and S4, and both the hydrodynamic size and PdI of LU in DM were significantly smaller than those in dispersed in distilled water. The zeta potential of all TiO_2 NPs dispersed in DM was negative and differed significantly from the values in distilled water. There were no differences in the zeta potential among the three TiO_2 NPs in DM. In cell culture medium, the values for hydrodynamic size and zeta potential were similar to those in DM. Specifically, the hydrodynamic size of S4 in cell culture medium was smaller than in DM.

Changes in body weight, organ weights, and lung histology

Body weight, major organ weights, and organ/body weight ratios were measured two weeks after exposure to TiO_2 NPs (Table 2). No significant changes in body weight, lung weight, and the lung/body weight ratio were detected between the control and exposure groups in the wild-type and Nrf2$^{-/-}$ mice. Similar findings were observed in adrenal glands and kidney. While the liver weight was significantly lower in the Nrf2$^{-/-}$ mice compared to the wild-type mice, no significant changes were evident at 14 days after exposure to all types of TiO_2 NPs in either strain. Although the weights of the heart and spleen tended to increase in Nrf2$^{-/-}$ mice compared to wild-type mice, no significant changes were observed in the exposure groups of both wild-type and Nrf2$^{-/-}$ mice when compared to the control group. In H&E-stained lung tissues, layers of inflammatory cells were not observed around bronchioles or blood vessels after exposure to TiO_2 NPs. Furthermore, no there were observable changes in alveolar size after exposure to TiO_2 NPs in either strain (data not shown).

Distribution of inflammatory cells and total protein in BALF

The total number of cells and the cell-type distribution were measured in BALF (Table 3). The total number of cells tended to increase at 14 days after exposure to 30 μg of all types of TiO_2 NPs in the wild-type and Nrf2$^{-/-}$ mice. However, no significant changes were observed in both mice. When compared to each control group, no significant changes were observed between the two mouse strains. Similar trends were observed in the distribution of macrophages, lymphocytes, and neutrophils, mirroring the findings of the total number of cells. Eosinophils were not observed in some of the TiO_2 NP exposure groups, and there was no significant change after exposure to

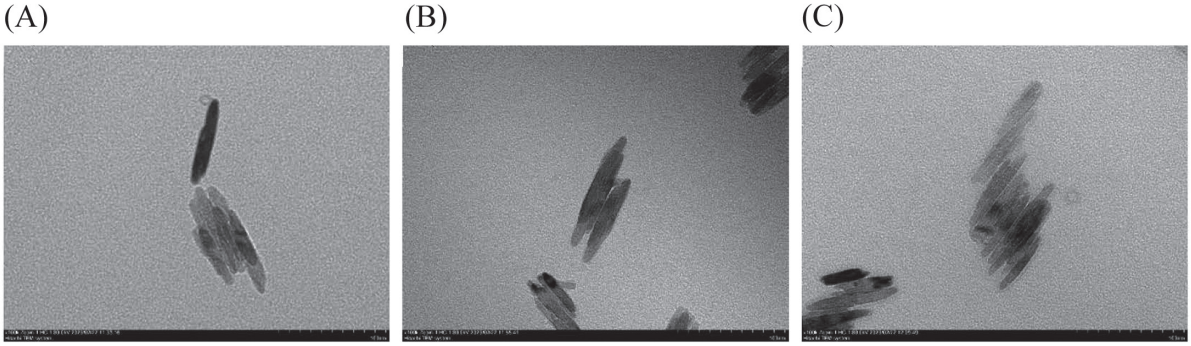

Fig. 1. Transmission electron microscope images of TiO_2 NPs. (A) LU-572-2 (LU), (B) TTO-S-3 (S3), and (C) TTO-S-4 (S4) (×100,000 magnification)

Table 1. Hydrodynamic size and zeta potential of TiO_2 NPs.

(A)

H_2O

Particles	Hydrodynamic size (nm)	PdI	Z-potential (mV)
LU	602.8 ± 161.1	0.515 ± 0.112	6.83 ± 0.40
S3	135.8 ± 2.82*	0.179 ± 0.019*	33.43 ± 0.84*
S4	145.8 ± 2.83*,†	0.183 ± 0.023*	30.5 ± 0.66*,†

(B)

DM

Particles	Hydrodynamic size (nm)	PdI	Z-potential (mV)
LU	106.7 ± 2.03‡	0.202 ± 0.001‡	-13.3 ± 0.64‡
S3	157.8 ± 1.79*,‡	0.151 ± 0.014*	-12.2 ± 0.81‡
S4	150.1 ± 1.22*,‡	0.145 ± 0.010*	-13.5 ± 2.23‡

(C)

Medium

Particles	Hydrodynamic size (nm)	PdI	Z-potential (mV)
LU	106.2 ± 3.43‡	0.407 ± 0.006‡	-11.2 ± 0.21‡
S3	140.2 ± 1.18*,‡	0.189 ± 0.005*	-11.5 ± 1.65‡
S4	137.2 ± 4.66*,†,‡,§	0.428 ± 0.078*	-10.2 ± 1.37‡

TiO_2 NPs were dispersed in each solvent. (A) shows the data dispersed in distilled water.
(B) shows the data dispersed in DM. (C) shows the data dispersed in cell culture medium.
Data are mean ± SD. PdI: Polydispersity Index. DLS measurements were repeated 3 times. *$p<0.05$, compared to LU in the same solvent. †$p<0.05$, compared to S3 in the same solvent. ‡$p<0.05$, compared to each TiO_2 NPs dispersed in distilled water. §$p<0.05$, compared to each TiO_2 NPs dispersed in DM. Tukey-kramer multiple comparison test following ANOVA.

all types of TiO_2 NPs in wild-type and $Nrf2^{-/-}$ mice. In addition, the total protein content of BALF remained unchanged after exposure to all types of TiO_2 NPs in both wild-type and $Nrf2^{-/-}$ mice.

Changes in mRNA levels in lung tissues

(a) Nrf2-related antioxidant protein

The mRNA expression of HO-1 and SOD-1 was not changed after exposure to all types of TiO_2 NPs in wild-type and $Nrf2^{-/-}$ mice, and there was no significant change between wild-type and $Nrf2^{-/-}$ mice (Table 4). NQO-1 mRNA expression was significantly lower in $Nrf2^{-/-}$ mice compared to wild-type mice in the control group, but no significant changes were observed between the control and exposure groups in either wild-type or $Nrf2^{-/-}$ mice (Table 4).

(b) Inflammatory cytokines

No significant changes were observed in the mRNA expression levels of IL-6 and TNFα between wild-type and $Nrf2^{-/-}$ mice in the control group (Table 4). Furthermore, the expression levels remained unchanged after exposure to all types of TiO_2 NPs in both wild-type and $Nrf2^{-/-}$ mice.

Cell viability and cytotoxicity in A549 cells

Cell viability was measured by MTS assay after administration of all types of TiO_2 NPs. The MTS assay results showed no changes in cell viability in A549 cells treated with all concentrations of TiO_2 NPs (Fig, 2). Furthermore, cytotoxicity was measured by LDH assay using supernatant collected before conducting the MTS assay. The LDH assay also showed no significant differences between the control group and all TiO_2 NP exposure groups (Fig. 3).

ROS measurements

Intracellular ROS levels were measured using the OxiSelect™ assay following exposure to all types of TiO_2 NPs at a concentration of 100 μg/mL (Fig. 4). Following exposure to S3 and S4 TiO_2 NPs, there was a tendency for ROS levels to increase in A549 cells at 3 hr after exposure compared to after 1 hr of exposure, but the production of ROS remained unchanged after exposure to LU TiO_2 NPs. After 6 or 12 hr of exposure to S4 and LU TiO_2 NPs, the production of ROS tended to decrease compared to 1 hour exposure period. Conversely, ROS levels remained elevated after exposure to S3 TiO_2 NPs. However, no significant differences were observed between the LU, S3, and S4 TiO_2 NP exposure groups at each time

Table 2. Body and organ weights of mice at 14 days after exposure to TiO_2 NPs.

	Genotype	Amount of TiO_2-NPs administered (μg)						
		0	LU		S3		S4	
			10	30	10	30	10	30
Body weight (g)	Wild-type	25.75 ± 0.89	25.63 ± 1.41	25.50 ± 0.76	25.88 ± 0.99	25.00 ± 1.60	25.13 ± 1.13	24.63 ± 1.77
	Nrf2 $^{-/-}$	28.17 ± 2.23	27.63 ± 1.92	27.56 ± 2.60	27.33 ± 1.58	27.22 ± 1.30	26.00 ± 1.50	27.50 ± 1.41
Lung weight (mg)	Wild-type	299.19 ± 20.42	308.68 ± 15.73	258.39 ± 41.78	305.51 ± 9.97	303.25 ± 22.36	292.09 ± 13.86	286.90 ± 19.95
	Nrf2 $^{-/-}$	346.65 ± 34.48	343.04 ± 22.36	333.83 ± 26.37	332.71 ± 35.01	318.89 ± 21.83	322.74 ± 14.18	343.80 ± 28.44
Lung weight/body weight ($\times 10^{-3}$)	Wild-type	11.62 ± 0.61	12.06 ± 0.46	10.16 ± 1.76	11.81 ± 0.35	12.18 ± 1.31	11.64 ± 0.58	11.66 ± 0.45
	Nrf2 $^{-/-}$	12.31 ± 0.70	12.43 ± 0.52	12.15 ± 0.74	12.17 ± 0.94	11.59 ± 0.67	12.43 ± 0.51	12.53 ± 1.29
Heart (mg)	Wild-type	118.56 ± 6.7	121.39 ± 10.21	116.69 ± 6.29	117.96 ± 6.43	116.00 ± 8.39	114.33 ± 12.59	116.58 ± 8.64
	Nrf2 $^{-/-}$	145.53 ± 19.49	152.39 ± 22.4	141.36 ± 18.65	139.81 ± 15.52	141.16 ± 13.26	132.81 ± 12.72	135.59 ± 15.85
Liver (mg)	Wild-type	1292.48 ± 136.26	1285.05 ± 208.09	1220.99 ± 117	1225.00 ± 142.68	1222.66 ± 129.68	1244.35 ± 115.43	1190.7 ± 118.44
	Nrf2 $^{-/-}$	1119.45 ± 160.62*	989.09 ± 102.46*	968.29 ± 171.59*	1051.94 ± 161.82*	994.77 ± 181.11*	981.36 ± 90.6*	1049.19 ± 156.94*
Spleen (mg)	Wild-type	56.33 ± 3.86	59.39 ± 2.51	58.64 ± 4.71	58.51 ± 4.50	58.04 ± 7.20	59.83 ± 5.4	61.21 ± 19.02
	Nrf2 $^{-/-}$	93.9 ± 38.35	100.74 ± 47.89	79.08 ± 22.27	81.27 ± 27.55	82.07 ± 29.18	67.72 ± 15.59	73.86 ± 14.42
Adrenal gland (mg)	Wild-type	6.03 ± 0.91	6.13 ± 1.78	5.96 ± 0.59	6.63 ± 1.97	5.81 ± 1.56	6.38 ± 1.85	5.08 ± 1.09
	Nrf2 $^{-/-}$	7.33 ± 1.61	6.53 ± 0.86	6.58 ± 1.48	7.16 ± 1.34	7.00 ± 1.12	6.82 ± 1.09	6.61 ± 1.05
Kidney (mg)	Wild-type	350.6 ± 19.10	354.7 ± 19.96	342.14 ± 28.03	357.96 ± 14.83	342.35 ± 13.88	332.99 ± 27.00	339.54 ± 28.04
	Nrf2 $^{-/-}$	390.97 ± 66.67	391.53 ± 54.42	351.07 ± 51.14	370.31 ± 51.11	359.79 ± 32.8	338.44 ± 34.35	358.33 ± 30.16

All data are mean ± SD. *$p<0.05$, compared to wild-type mice exposed to each TiO_2 NPs, by student t-test.

Table 3. Total number of cells, distribution of inflammatory cells, and total protein levels in BALF.

	Genotype	Amount of TiO_2 NPs administered (μg)						
		0	LU		S3		S4	
			10	30	10	30	10	30
Total cells ($\times 10^4$)	Wild-type	13.1 ± 4.8	16.1 ± 2.9	15.3 ± 4.0	14.7 ± 1.9	15.0 ± 3.3	20.2 ± 7.0	17.6 ± 3.8
	Nrf2 $^{-/-}$	13.4 ± 3.4	13.7 ± 5.1	16.3 ± 2.8	13.2 ± 3.5	14.9 ± 4.1	13.3 ± 4.8	15.1 ± 3.8
Macrophages ($\times 10^4$)	Wild-type	12.9 ± 4.7	15.7 ± 2.8	14.9 ± 3.9	14.5 ± 1.9	14.6 ± 3.2	19.4 ± 5.9	17.1 ± 3.4
	Nrf2 $^{-/-}$	12.8 ± 3.1	13.0 ± 4.8	16.1 ± 2.8	12.9 ± 3.5	14.5 ± 4.0	13.1 ± 4.7	14.7 ± 3.5
Lymphocytes ($\times 10^4$)	Wild-type	0.2 ± 0.2	0.3 ± 0.6	0.4 ± 0.5	0.2 ± 0.08	0.3 ± 0.2	0.5 ± 1.1	0.3 ± 0.2
	Nrf2 $^{-/-}$	0.4 ± 0.6	0.4 ± 0.6	0.2 ± 0.2	0.3 ± 0.2	0.3 ± 0.2	0.08 ± 0.09	0.3 ± 0.4
Neutrophiles ($\times 10^4$)	Wild-type	0.04 ± 0.05	0.07 ± 0.08	0.07 ± 0.06	0.04 ± 0.06	0.06 ± 0.07	0.15 ± 0.07	0.14 ± 0.28
	Nrf2 $^{-/-}$	0.04 ± 0.06	0.25 ± 0.38	0.01 ± 0.03	0.08 ± 0.09	0.07 ± 0.07	0.08 ± 0.10	0.05 ± 0.19
Eosinophiles ($\times 10^4$)	Wild-type	0.01 ± 0.02	0	0	0	0	0.13 ± 0.33	0.15 ± 0.56
	Nrf2 $^{-/-}$	0.03 ± 0.05	0.01 ± 0.01	0	0.02 ± 0.06	0.01 ± 0.02	0	0.05 ± 0.19
Total protein (μg/mL)	Wild-type	127.81 ± 25.81	134.19 ± 9.28	128.04 ± 19.69	129.31 ± 23.79	130.26 ± 18.73	120.21 ± 20.03	136.89 ± 26.54
	Nrf2 $^{-/-}$	126.82 ± 23.74	114.93 ± 26.53	116.72 ± 17.05	127.21 ± 25.8	122.33 ± 30.45	120.46 ± 11.98	121.08 ± 16.58

All data are mean ± SD.

Table 4. Relative mRNA expression levels of Nrf2-related proteins and inflammatory cytokines.

	Genotype	Amount of TiO_2-NPs administered (μg)						
		0	LU		S3		S4	
			10	30	10	30	10	30
HO-1	Wild-type	0.08 ± 0.03	0.09 ± 0.05	0.09 ± 0.07	0.10 ± 0.08	0.08 ± 0.07	0.10 ± 0.07	0.10 ± 0.07
	Nrf2 $^{-/-}$	0.05 ± 0.02	0.09 ± 0.06	0.07 ± 0.03	0.07 ± 0.04	0.08 ± 0.04	0.07 ± 0.05	0.07 ± 0.05
NQO-1	Wild-type	2.3 ± 1.1	2.2 ± 1.2	2.4 ± 0.6	3.7 ± 2.6	2.3 ± 0.5	2.1 ± 0.8	2.6 ± 1.5
	Nrf2 $^{-/-}$	0.5 ± 0.2*	0.5 ± 0.3*	0.9 ± 0.4*	0.3 ± 0.2*	0.4 ± 0.3*	0.3 ± 0.2*	0.3 ± 0.3*
SOD-1	Wild-type	0.7 ± 0.3	0.8 ± 0.3	0.8 ± 0.4	0.8 ± 0.5	0.8 ± 0.5	0.8 ± 0.4	0.9 ± 0.6
	Nrf2 $^{-/-}$	0.5 ± 0.3	0.7 ± 0.4	0.8 ± 0.4	0.6 ± 0.2	0.8 ± 0.4	0.7 ± 0.2	0.6 ± 0.3
IL-6	Wild-type	0.3 ± 0.1	0.4 ± 0.4	0.3 ± 0.3	0.4 ± 0.4	0.4 ± 0.4	0.3 ± 0.3	0.3 ± 0.2
	Nrf2 $^{-/-}$	0.3 ± 0.2	0.4 ± 0.2	0.4 ± 0.4	0.1 ± 0.06	0.2 ± 0.07	0.2 ± 0.1	0.2 ± 0.1
TNFα	Wild-type	1.4 ± 0.9	1.6 ± 1.0	1.3 ± 0.9	1.5 ± 1.2	0.8 ± 0.5	0.8 ± 0.4	1.1 ± 0.9
	Nrf2 $^{-/-}$	2.1 ± 1.3	2.7 ± 2.2	2.2 ± 1.7	3.1 ± 2.1	2.1 ± 1.2	3.3 ± 2.9	2.6 ± 1.8

All data are mean ± SD. *$p<0.05$, compared to wild-type mice exposed to each TiO_2 NPs, by student t-test.

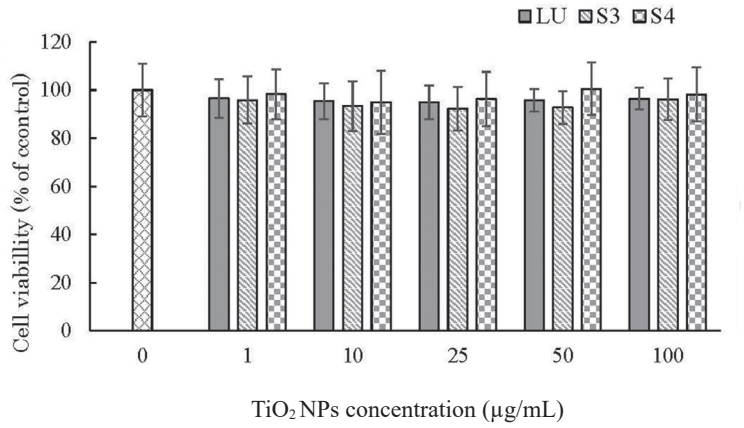

Fig. 2. Effect of TiO_2 NPs on cell viability in A549 cells. Cell viability was measured by the MTS assay. A549 cells were exposed to tree types of TiO_2 NPs at concentrations of 0, 1, 10, 25, 50, and 100 μg/mL for 24 hr. All data are mean ± SD.

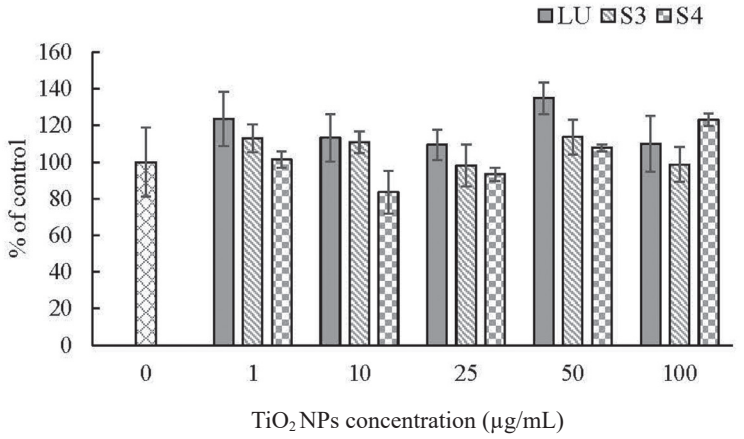

Fig. 3. Effect of TiO_2 NPs on cytotoxicity in A549 cells. Cytotoxicity was measured by the LDH assay. A549 cells were exposed to three types of TiO_2 NPs at concentrations of 0, 1, 10, 25, 50, and 100 μg/mL for 24 hr. All data are mean ± SD.

point of measurement.

DISCUSSION

The present study investigated the effects of exposure to TiO_2 NPs with three different surface coatings both *in vivo* (in wild-type and Nrf2 null mice) and *in vitro* (using alveolar epithelial cells). Our results show that the surface coatings on the TiO_2 NPs did not influence pulmonary outcomes in either the mouse models or the A549 cell line.

TiO_2 NPs are known to exist in three crystalline forms: rutile, anatase, and brookite (Thakur *et al*., 2024). Previous studies have shown that anatase TiO_2 NPs exhibit higher photocatalytic activity and induce more pronounced biological effects compared to rutile TiO_2 NPs (Sayes *et al*., 2006; Tada-Oikawa *et al*., 2016). In the present study, we used rutile TiO_2 NPs due to their relative-

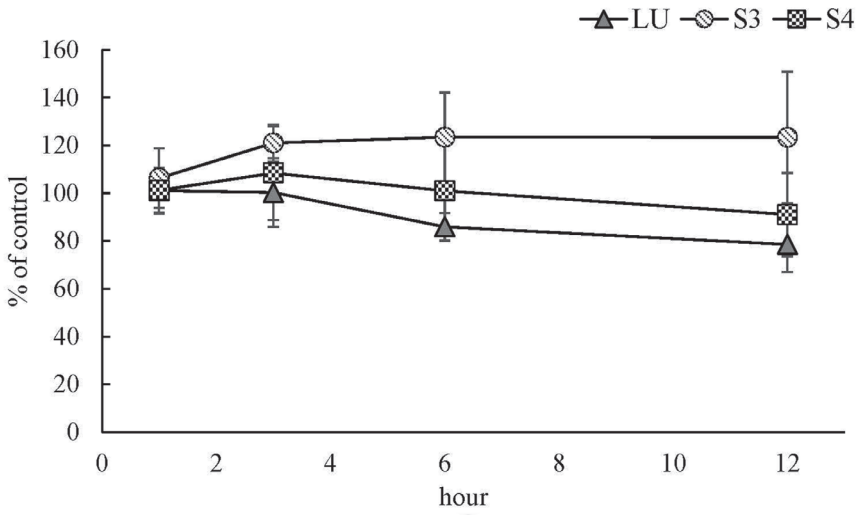

Fig. 4. ROS generation in A549 cells. Intracellular ROS was measured using an Oxiselect™ kit. A549 cells were exposed to three types of TiO_2 NPs at concentrations of 100 μg/mL. ROS was measured at 1, 3, 6, and 12 hr. All data are mean ± SD.

ly minimal biological impact, which allows for a clearer assessment of the effects of surface coating modifications on biological responses. Additionally, TiO_2 NPs can vary in shape (i.e., spherical, fibrous, and spindle-shaped forms), which influences their dispersion in solutions and toxicity profiles (Thakur *et al*., 2024). For example, spherical nanoparticles have been reported to induce oxidative stress and DNA single-strand breaks in A549 cells (Jugan *et al*., 2012), and nanobelts longer than 15 nm have been associated with inflammation in lung alveoli, similar to asbestos or silica (Hamilton *et al*., 2009; Wang and Fan, 2014). Conversely, spindle-shaped nanoparticles, which have smaller aggregate sizes and more stable dispersion characteristics in solvents compared to spherical nanoparticles (Konstantinova *et al*., 2017), have been shown to exhibit lower uptake into fibroblasts (Allouni *et al*., 2012). The spindle-shaped TiO_2 NPs used in the present study, characterized by their stability and lower biological interaction, are thus considered to be safer for products such as cosmetics and sunscreens. Furthermore, the TEM analysis in the present study confirmed that these spindle-shaped TiO_2 NPs retained their shape after surface coating. Given the absence of shape alterations, our study focused on the biological effects of the different surface coatings on these NPs.

TiO_2 NPs are used in sunscreens due to their high transparency and UV absorption properties. Given that the surface coatings on TiO_2 NPs can markedly affect their solubility, stability, and reactivity (Thakur *et al*., 2024; Wang and Fan, 2014), these surface coatings are widely used for specific applications in products. For example, a previous study showed that exposure to TiO_2 NPs coated with amorphous silica and/or aluminum oxide caused lung inflammation in rats compared to TiO_2 NPs without a surface coating (Warheit *et al*., 2005). Another study showed that lung cancer cells exposed to TiO_2 NPs with -OH, $-NH_2$, and -COOH coatings showed an increase in cell viability, especially in the treatment using TiO_2 NPs with a -COOH surface coating, compared to TiO_2 NPs without surface coating (Thevenot *et al*., 2008). These effects are considered to be influenced not only by the inherent toxicity of the surface coating itself, but also by changes in cellular uptake affected by the surface coatings. Furthermore, a study by Rossi *et al*. (2010) showed that exposure to TiO_2 NPs coated with silica not only caused lung inflammation, but also increased levels of TNF-α and the chemokine CXCL1, compared to TiO_2 NPs without a surface coating. Thus, there is concern that inflammation is attributed to the toxicity of the surface coating itself. In the present study, the TiO_2 NPs used were coated with aluminum hydroxide and aluminum hydroxide/stearic acid. These coated TiO_2 NPs are widely used as ingredients in sunscreens (Ishihara Sangyo Kaisha, Osaka, Japan, https://www.iskweb.co.jp/products/

functional02.html). Other TiO_2 NPs with aluminum hydroxide or stearic acid surface coatings are also used as ingredients in cosmetics and sunscreens. Given that TiO_2 NPs with surface coatings are already being used extensively in products around the world, evaluating their potential toxicity is important.

Aluminum is widely used in cosmetics and as a vaccine adjuvant. The acute toxicity of aluminum hydroxide, particularly to the respiratory system, is considered to be minimal due to its low absorption rate (Chang *et al*., 2016; Krewski *et al*., 2007). However, the toxicity of aluminum hydroxide is influenced by renal function; for example, in uremic animals, symptoms such as lethargy, periorbital bleeding, anorexia, and death have been reported, and deposition in brain, liver, heart, and muscle has also been observed (Krewski *et al*., 2007). The S3 TiO_2 NPs used in the present study were coated with aluminum hydroxide. The results indicated that there were no significant changes in inflammatory responses or mRNA expression in the lungs of mice treated with S3 NPs, nor in cell viability or cytotoxicity in A549 cells. Similarly, the S4 TiO_2 NPs were coated with both aluminum hydroxide and stearic acid, a fatty acid commonly found in cosmetic-grade TiO_2 NPs. A previous study showed that TiO_2 NPs coated with a mixture of various fatty acids (i.e., palmitoleic acid, palmitic acid, stearic acid, and oleic acid) can inhibit cell death (Chang *et al*., 2016). In the present study, no inflammation or cytotoxicity was observed in the lungs of mice treated with S4 NPs, which is consistent with the findings of previous studies.

Surface coatings have been demonstrated to alter the physicochemical properties of NPs, affecting their cellular uptake and intracellular activities (Wilhelm *et al*., 2003). Zeta potential, in particular, has been implicated in the modulation of cellular uptake mechanisms. Nanosized drug carriers possessing negative zeta potential have shown an enhanced ability to pass through the mucus layer due to electrostatic repulsion, whereas nanocarriers with a positive zeta potential are readily taken up by cells (Sharifi *et al*., 2021). Of the three types of TiO_2 NPs used in the present study, all exhibited positive zeta potential in distilled water, but displayed negative zeta potential in highly buffered solutions, such as DM and cell culture medium. Notably, the zeta potential values did not change in DM and in cell culture medium. This result suggests that although the zeta potential values differed among the three TiO_2 NPs with different surface coatings in distilled water, these differences did not markedly affect the induction of inflammatory responses by the TiO_2 NPs.

We also investigated the influence of Nrf2 on exposure to TiO_2 NPs with different surface coatings. A previous study showed that aspiration of ZnO NPs led to an increase in total cell counts, macrophages, lymphocytes, and eosinophils in BALF in both wild-type and $Nrf2^{-/-}$ mice, with a more pronounced increase observed in $Nrf2^{-/-}$ mice (Sehsah *et al*., 2019). However, in our study, despite employing the same exposure concentration as that for ZnO NPs, the total cell count in BALF remained unchanged in both wild-type and $Nrf2^{-/-}$ mice following TiO_2 NP exposure. This finding suggests that TiO_2 NPs in the lung are comparatively less toxic than ZnO NPs.

In addition, the current investigation measured the mRNA expression levels of inflammatory cytokines and antioxidant stress response factors in lung tissues. NPs are known to induce inflammation via oxidative stress, and it has been shown that anatase-type TiO_2 NPs can elevate reactive oxygen species and cause inflammation (Sayes *et al*., 2006). In our study, there was a tendency for intracellular ROS levels to increase in the S3 TiO_2 NP exposure group, but there was no significant difference compared to the other TiO_2 NPs tested. In addition, no significant changes were observed in the mRNA expression levels of inflammatory cytokines and antioxidant stress response factors in lung tissues of $Nrf2^{-/-}$ mice, despite the observed increase in ROS production associated with changes in surface coating. These findings collectively suggest that while ROS production tends to increase in response to changes in the surface coating, such changes were insufficient to elicit discernable biological effects or induce changes in mRNA expression levels of antioxidant stress response factors.

In conclusion, modifying the surface coating of NPs can increase the potential health risks associated with their toxicity. However, in the context of our study, the examined TiO_2 NPs showed no discernable biological effects on the lung. Specifically, rutile TiO_2 NPs coated with aluminum hydroxide or a combination of aluminum hydroxide and stearic acid demonstrated low toxicity profiles.

ACKNOWLEDGMENTS

The authors thank the company (Ishihara Sangyo Kaisha, Osaka, Japan) for providing TiO_2 NPs. We also thank Akane Sakakibara and Yumiko Tateno for their assistance with manuscript preparation.

Conflict of interest---- The authors declare that there is no conflict of interest.

REFERENCES

Allouni, Z.E., Hol, P.J., Cauqui, M.A., Gjerdet, N.R. and Cimpan, M.R. (2012): Role of physicochemical characteristics in the uptake of TiO_2 nanoparticles by fibroblasts. Toxicol. In Vitro, **26**, 469-479.

Bampidis, V., Azimonti, G., Bastos, M.L., Christensen, H., Dusemund, B., Fašmon Durjava, M., Kouba, M., López-Alonso, M., López Puente, S., Marcon, F., Mayo, B., Pechová, A., Petkova, M., Ramos, F., Sanz, Y., Villa, R.E., Woutersen, R., Aquilina, G., Bories, G., Gropp, J., Galobart, J. and Vettori, M.V. (2021): Safety and efficacy of a feed additive consisting of titanium dioxide for all animal species (Titanium Dioxide Manufacturers Association). EFSA J., **19**, e06630.

Baranowska-Wojcik, E., Szwajgier, D., Oleszczuk, P. and Winiarska-Mieczan, A. (2020): Effects of titanium dioxide nanoparticles exposure on human health-a review. Biol. Trace Elem. Res., **193**, 118-129.

Bellezza, I., Giambanco, I., Minelli, A. and Donato, R. (2018): Nrf2-Keap1 signaling in oxidative and reductive stress. Biochim. Biophys. Acta Mol. Cell Res., **1865**, 721-733.

Bettini, S., Boutet-Robinet, E., Cartier, C., Comera, C., Gaultier, E., Dupuy, J., Naud, N., Tache, S., Grysan, P., Reguer, S., Thieriet, N., Refregiers, M., Thiaudiere, D., Cravedi, J.P., Carriere, M., Audinot, J.N., Pierre, F.H., Guzylack-Piriou, L. and Houdeau, E. (2017): Food-grade TiO2 impairs intestinal and systemic immune homeostasis, initiates preneoplastic lesions and promotes aberrant crypt development in the rat colon. Sci. Rep., **7**, 40373.

Bhattacharjee, S. (2016): DLS and zeta potential - What they are and what they are not? J. Control. Release, **235**, 337-351.

Chang, J., Lee, C.W., Alsulimani, H.H., Choi, J.E., Lee, J.K., Kim, A., Park, B.H., Kim, J. and Lee, H. (2016): Role of fatty acid composites in the toxicity of titanium dioxide nanoparticles used in cosmetic products. J. Toxicol. Sci., **41**, 533-542.

Chaudhry, Q., Scotter, M., Blackburn, J., Ross, B., Boxall, A., Castle, L., Aitken, R. and Watkins, R. (2008): Applications and implications of nanotechnologies for the food sector. Food Addit. Contam. Part A Chem. Anal. Control Expo. Risk Assess., **25**, 241-258.

De Stefano, D., Carnuccio, R. and Maiuri, M.C. (2012): Nanomaterials toxicity and cell death modalities. J. Drug Deliv., **2012**, 167896.

Hamilton, R.F., Wu, N., Porter, D., Buford, M., Wolfarth, M. and Holian, A. (2009): Particle length-dependent titanium dioxide nanomaterials toxicity and bioactivity. Part. Fibre Toxicol., **6**, 35.

Ichihara, S., Li, W., Omura, S., Fujitani, Y., Liu, Y., Wang, Q., Hiraku, Y., Hisanaga, N., Wakai, K., Ding, X., Kobayashi, T. and Ichihara, G. (2016): Exposure assessment and heart rate variability monitoring in workers handling titanium dioxide particles: a pilot study. J. Nano Res., **18**, 52.

Inoue, M., Sakamoto, K., Suzuki, A., Nakai, S., Ando, A., Shiraki, Y., Nakahara, Y., Omura, M., Enomoto, A., Nakase, I., Sawada, M. and Hashimoto, N. (2021): Size and surface modification of silica nanoparticles affect the severity of lung toxicity by modulating endosomal ROS generation in macrophages. Part. Fibre Toxicol., **18**, 21.

Itoh, K., Chiba, T., Takahashi, S., Ishii, T., Igarashi, K., Katoh, Y., Oyake, T., Hayashi, N., Satoh, K., Hatayama, I., Yamamoto, M. and Nabeshima, Y. (1997): An Nrf2/small Maf heterodimer mediates the induction of phase II detoxifying enzyme genes through antioxidant response elements. Biochem. Biophys. Res. Commun., **236**, 313-322.

Johnson, N.M., Hoffmann, A.R., Behlen, J.C., Lau, C., Pendleton, D., Harvey, N., Shore, R., Li, Y., Chen, J., Tian, Y. and Zhang, R. (2021): Air pollution and children's health-a review of adverse effects associated with prenatal exposure from fine to ultrafine particulate matter. Environ. Health Prev. Med., **26**, 72.

Jugan, M.-L., Barillet, S., Simon-Deckers, A., Herlin-Boime, N., Sauvaigo, S., Douki, T. and Carriere, M. (2012): Titanium dioxide nanoparticles exhibit genotoxicity and impair DNA repair activity in A549 cells. Nanotoxicology, **6**, 501-513.

Konstantinova, V., Ibrahim, M., Lie, S.A., Birkeland, E.S., Neppelberg, E., Marthinussen, M.C., Costea, D.E. and Cimpan, M.R. (2017): Nano-TiO(2) penetration of oral mucosa: *in vitro* analysis using 3D organotypic human buccal mucosa models. J. Oral Pathol. Med., **46**, 214-222.

Krewski, D., Yokel, R. A., Nieboer, E., Borchelt, D., Cohen, J., Harry, J., Kacew, S., Lindsay, J., Mahfouz, A. M. and Rondeau, V. (2007): Human health risk assessment for aluminium, aluminium oxide, and aluminium hydroxide. J Toxicol Environ Health B Crit Rev, 10 Suppl 1(Suppl 1), 1-269.

Najahi-Missaoui, W., Arnold, R.D. and Cummings, B.S. (2020): Safe Nanoparticles: are we there yet? Int. J. Mol. Sci., **22**, 385.

Piccinno, F., Gottschalk, F., Seeger, S. and Nowack, B. (2012): Industrial production quantities and uses of ten engineered nanomaterials in Europe and the world. J. Nano Res., **14**, 1109.

Rossi, E.M., Pylkkanen, L., Koivisto, A.J., Vippola, M., Jensen, K.A., Miettinen, M., Sirola, K., Nykasenoja, H., Karisola, P., Stjernvall, T., Vanhala, E., Kiilunen, M., Pasanen, P., Makinen, M., Hameri, K., Joutsensaari, J., Tuomi, T., Jokiniemi, J., Wolff, H., Savolainen, K., Matikainen, S. and Alenius, H. (2010): Airway exposure to silica-coated TiO_2 nanoparticles induces pulmonary neutrophilia in mice. Toxicol. Sci., **113**, 422-433.

Sayes, C.M., Wahi, R., Kurian, P.A., Liu, Y., West, J.L., Ausman, K.D., Warheit, D.B. and Colvin, V.L. (2006): Correlating nanoscale titania structure with toxicity: a cytotoxicity and inflammatory response study with human dermal fibroblasts and human lung epithelial cells. Toxicol. Sci., **92**, 174-185.

Sehsah, R., Wu, W., Ichihara, S., Hashimoto, N., Hasegawa, Y., Zong, C., Itoh, K., Yamamoto, M., Elsayed, A.A., El-Bestar, S., Kamel, E. and Ichihara, G. (2019): Role of Nrf2 in inflammatory response in lung of mice exposed to zinc oxide nanoparticles. Part. Fibre Toxicol., **16**, 47.

Sehsah, R., Wu, W., Ichihara, S., Hashimoto, N., Zong, C., Yamazaki, K., Sato, H., Itoh, K., Yamamoto, M., Elsayed, A.A., El-Bestar, S., Kamel, E. and Ichihara, G. (2022): Protective role of Nrf2 in zinc oxide nanoparticles-induced lung inflammation in female mice and sexual dimorphism in susceptibility. Toxicol. Lett., **370**, 24-34.

Sharifi, F., Jahangiri, M., Nazir, I., Asim, M.H., Ebrahimnejad, P., Hupfauf, A., Gust, R. and Bernkop-Schnurch, A. (2021): Zeta potential changing nanoemulsions based on a simple zwitterion. J. Colloid Interface Sci., **585**, 126-137.

Shi, Z., Niu, Y., Wang, Q., Shi, L., Guo, H., Liu, Y., Zhu, Y., Liu, S., Liu, C., Chen, X. and Zhang, R. (2015): Reduction of DNA damage induced by titanium dioxide nanoparticles through Nrf2 *in vitro* and *in vivo*. J. Hazard. Mater., **298**, 310-319.

Suttiponparnit, K., Jiang, J., Sahu, M., Suvachittanont, S., Charinpanitkul, T. and Biswas, P. (2011): Role of surface area, primary particle size, and crystal phase on titanium dioxide nanoparticle dispersion properties. Nanoscale Res. Lett., **6**, 27.

Suzuki, Y., Tada-Oikawa, S., Hayashi, Y., Izuoka, K., Kataoka, M., Ichikawa, S., Wu, W., Zong, C., Ichihara, G. and Ichihara, S. (2016) Single- and double-walled carbon nanotubes enhance atherosclerogenesis by promoting monocyte adhesion to endothelial cells and endothelial progenitor cell dysfunction. Part. Fibre Toxicol., **13**, 54.

Tada-Oikawa, S., Ichihara, G., Fukatsu, H., Shimanuki, Y., Tanaka, N., Watanabe, E., Suzuki, Y., Murakami, M., Izuoka, K., Chang, J., Wu, W., Yamada, Y. and Ichihara, S. (2016): Titanium dioxide particle type and concentration influence the inflammatory response in caco-2 cells. Int. J. Mol. Sci., **17**, 576.

Takechi-Haraya, Y., Ohgita, T., Demizu, Y., Saito, H., Izutsu, K.I. and Sakai-Kato, K. (2022): Current status and challenges of analytical methods for evaluation of size and surface modification of nanoparticle-based drug formulations. AAPS PharmSciTech, **23**, 150.

Thakur, N., Thakur, N., Kumar, A., Thakur, V.K., Kalia, S., Arya, V., Kumar, A., Kumar, S. and Kyzas, G.Z. (2024): A critical review on the recent trends of photocatalytic, antibacterial, antioxidant and nanohybrid applications of anatase and rutile TiO_2 nanoparticles. Sci. Total Environ., **914**, 169815.

Thangavel, P., Park, D. and Lee, Y.C. (2022): Recent insights into particulate matter (PM(2.5)-mediated toxicity in humans: an overview. Int. J. Environ. Res. Public Health, **19**, 7571.

Thevenot, P., Cho, J., Wavhal, D., Timmons, R.B. and Tang, L. (2008): Surface chemistry influences cancer killing effect of TiO_2 nanoparticles. Nanomedicine (Lond.), **4**, 226-236.

Wang, J. and Fan, Y. (2014): Lung injury induced by TiO_2 nanoparticles depends on their structural features: Size, shape, crystal phases, and surface coating. Int. J. Mol. Sci., **15**, 22258-22278.

Warheit, D.B., Brock, W.J., Lee, K.P., Webb, T.R. and Reed, K.L. (2005): Comparative pulmonary toxicity inhalation and instillation studies with different TiO_2 particle formulations: impact of surface treatments on particle toxicity. Toxicol. Sci., **88**, 514-524.

Wilhelm, C., Billotey, C., Roger, J., Pons, J.N., Bacri, J.C. and Gazeau, F. (2003): Intracellular uptake of anionic superparamagnetic nanoparticles as a function of their surface coating. Biomaterials, **24**, 1001-1011.

Wu, W., Ichihara, G., Suzuki, Y., Izuoka, K., Oikawa-Tada, S., Chang, J., Sakai, K., Miyazawa, K., Porter, D., Castranova, V., Kawaguchi, M. and Ichihara, S. (2014): Dispersion method for safety research on manufactured nanomaterials. Ind. Health, **52**, 54-65.

Yoshida, T., Yoshioka, Y., Matsuyama, K., Nakazato, Y., Tochigi, S., Hirai, T., Kondoh, S., Nagano, K., Abe, Y., Kamada, H., Tsunoda, S., Nabeshi, H., Yoshikawa, T. and Tsutsumi, Y. (2012): Surface modification of amorphous nanosilica particles suppresses nanosilica-induced cytotoxicity, ROS generation, and DNA damage in various mammalian cells. Biochem. Biophys. Res. Commun., **427**, 748-752.

Zhang, R., Niu, Y., Li, Y., Zhao, C., Song, B., Li, Y. and Zhou, Y. (2010): Acute toxicity study of the interaction between titanium dioxide nanoparticles and lead acetate in mice. Environ. Toxicol. Pharmacol., **30**, 52-60.

Zhang, S., Gao, H. and Bao, G. (2015): Physical principles of nanoparticle cellular endocytosis. ACS Nano, **9**, 8655-8671.